

Experimental Study and Analysis of Slip Damping in Multilayer Bolted Cantilever Beam

Shaitan Singh¹ Prof.A.K.Jain²

¹Researcher ²Professor

^{1,2}Department of Mechanical Engineering

^{1,2}Jabalpur Engineering College Jabalpur, India

Abstract— Bolted joints are often used to fabricate assembled structures in machine tools, automotive and many such industries requiring high damping. Vibration attenuation in these structures can enhance the dynamic stability significantly. A little amount of work has been reported till date on the damping capacity of bolted structures. The present work outlines the basic formulation for the slip damping mechanism in multilayered and bolted structures, vibrating under dynamic conditions. The numerical stability of the method and its applicability to actual working conditions have been investigated in the case of a bolted cantilever beam structure with multiple interfaces. The developed damping model of the structure is found to be fairly in good agreement with experimental data.

Key words: Multilayer Bolted Cantilever Beam, Slip Damping

I. INTRODUCTION

With the increasing use of bolted, welded and riveted layered beams as structural members there has been a critical need for development of reliable and practical mathematical models to predict the dynamic behavior of such built-up structures. Joints are inherently present in almost all assembled structures which contribute significantly to the slip damping. Joints have a great potential to reduce the vibration levels thereby attracting the interest of many researchers. In an earlier attempt, theory of structural damping in a built-up beam has been investigated by Pian and Hallowell [4] considering the beam being fabricated in two parts and connected by riveted cover plates. Goodman and Klumpp [6] examined the energy dissipation by slip at the interfaces of a laminated beam. In fact, investigators such as Cockerham and Symons [8], Hess et al. [7] and Guyan et al. [9] considered various friction and excitation models, while Barnett et al. [10] and Maugin et al. [11] considered interfacial slip waves between two surfaces for the measurement of damping capacity of these structures. Hansen and Spies [12] investigated the structural damping in laminated beams due to interfacial slip. They analyzed a two layered plate model with an assumption that there exists an adhesive layer of negligible thickness and mass between the two layers such that some amount of micro-slip originates at the frictional interfaces which contributes to the slip damping. They have also shown that the restoring force is developed by this adhesive medium and is proportional to the interfacial micro-slip. Recently, Damisa et al. [13] examined the effect of linear interface pressure distribution on the mechanism of slip damping for layered beams vibrating at static conditions. However, Olunloyo et al. [14] in their analysis on slip damping of clamped beams included other forms of interfacial pressure distributions such as polynomial or hyperbolic expressions. Though these researchers

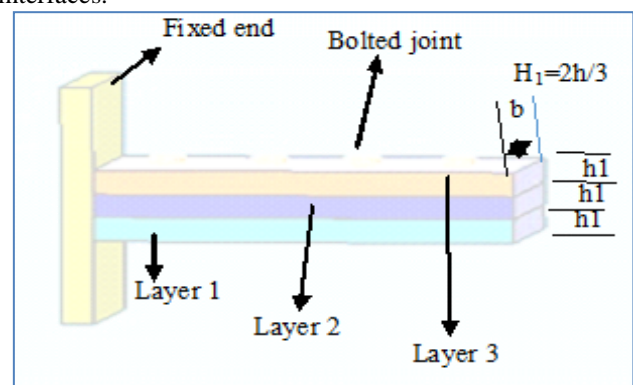
considered the in-plane distribution of bending stresses but all the analysis is limited to the structures with single interface. They did not consider the effect of multiple interfaces on the damping capacity of these structures. However Bhagat Singh and B. K. Nanda [1] extended this work taking multi interfaces by welding different interfaces.

In the present paper the work of Bhagat Singh and B.K. Nanda is carried out in multilayered beam with bolted joints. The objective of the present work is to develop a mathematical model to estimate the damping capacity of bolted structures with multiple interfaces. The problem is idealized as a multilayered and bolted beam model, vibrating at dynamic conditions. The beam is cantilevered from one end. Experiments are performed on mild steel specimens with a number of layers under different initial conditions of excitation to validate the theory developed. It is observed that a considerable increase in damping capacity can be achieved by increasing the number of layers.

II. THEORETICAL ANALYSIS

A. Static Analysis

To study the mechanism of slip damping in multilayered built up structures with multiple interfaces, the bolted cantilever beam model as shown in Fig. 1(a) is considered with overall thickness $2h$, width b , length l and made up of 'm' number of laminates of equal thickness ($2h/m$), so that the slip is occurring on $(m - 1)$ number of interfaces simultaneously. The loading consists of uniformly distributed pressure at the interfaces due to contact between flat bodies, and a concentrated load P applied at the free end, $x = l$. The continuity of stress and vertical displacement 'v' is imposed at the interfaces. Each of the laminates of thickness $2h/m$ is considered separately with the loading as depicted in Fig. 1(b). At some finite value of P , the shear stress at the interfaces will reach the critical value for slip $\tau_{xy} = \mu p$ where μ and p are the kinematic coefficient of friction and interface pressure, respectively. Additional static force due to excitation will produce a relative displacement $u(x)$ at the interfaces.



(a)

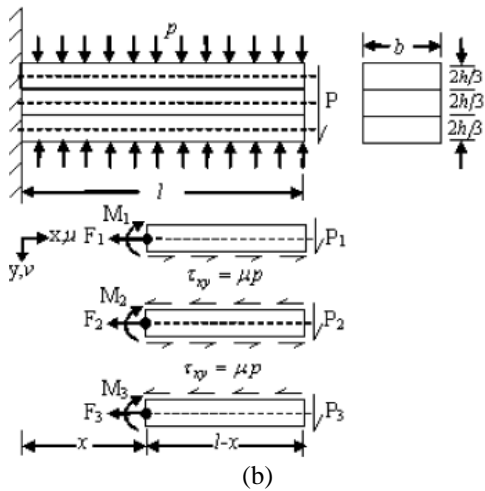


Fig. 1(a): Three layered tack welded cantilever beam model.
(b) Three layers of the jointed beam depicting load and coordinates.

1) Interface pressure distribution

The contact pressure for flat surfaces with rounded corners has been found out by Ciavarella et al., which shows a non-uniform distribution pattern at the interfaces. Contrary to this, the pressure distribution at the interfaces is assumed to be uniform owing to the contact of the upper layer over the lower one. In the present analysis, the welded beams are perfectly flat and the relation for uniform pressure distribution as given by Johnson[15] and Giannakopoulos et al.[16] due to contact of two flat bodies has been considered and the same is given by

$$p(x) = \frac{P}{b} \quad (1)$$

Where, P and b are the normal load per unit length and width of the beam respectively.

2) Analysis of static response

The resultant bending moment about the centroid of each laminate as shown in Fig.1(b) is found to be:

$$M_m = \frac{1}{m} \left[p \frac{2(m-1)\mu p b h}{m} \right] (1-x) \quad (2)$$

Invoking the relation between bending moment and curvature as derived by Warburton[17], we get:

$$M = -EI \frac{d^2 v}{dx^2} \quad (3)$$

Where E is the modulus of elasticity.

Putting expression (3) in (2) the following expression is obtained:

$$\frac{d^2 v}{dx^2} = \frac{1}{mEI} \left[p \frac{2(m-1)\mu p b h}{m} \right] (1-x) \quad (4)$$

Where $I = b \left(\frac{2h}{3}\right)^3 / 12$ is the moment of inertia of the cross-section of the beam.

Integrating expression (4) once we get:

$$\frac{dv}{dx} = \frac{3m^2}{2Ebh^3} \left[p \frac{2(m-1)\mu p b h}{m} \right] \left(lx - \frac{x^2}{2} \right) + C_1 \quad (5)$$

Where C_1 is the integration constant and evaluated to be zero by putting the boundary condition $(dv/dx)|_{x=0} = 0$ in the expression (5).

Further, integration of expression (5) yields:

$$\frac{dv}{dx} = \frac{3m^2}{2Ebh^3} \left[p \frac{2(m-1)\mu p b h}{m} \right] \left(\frac{lx^2}{2} - \frac{x^3}{6} \right) + C_2 \quad (6)$$

Putting the value of C_2 in the expression (6) and simplifying, the static deflection mode shape is given by

$$V = \frac{l^3}{Ebh^3} \left[p \frac{2(m-1)\mu p b h}{m} \right] \left[\frac{3m^2}{4} \left(\frac{x}{l} \right)^2 - \frac{m^2}{4} \left(\frac{x}{l} \right)^3 \right] \quad (7)$$

The two dimensional parameters Q and R are defined as presented Below

$$Q = \mu p b h \quad (8a)$$

$$R = \frac{E b h^3}{l^3} \quad (8b)$$

Putting the values of Q and R in equation 7 and simplifying we get:

$$V = \frac{1}{R} \left[p \frac{2(m-1)Q}{m} \right] \left[\frac{3m^2}{4} \left(\frac{x}{l} \right)^2 - \frac{1}{4} \left(\frac{x}{l} \right)^3 \right] \quad (9)$$

B. Dynamic Analysis

1) Analysis of Dynamic Response

The forced vibration of the beam produced by a time-dependent displacement at the unsupported end has been considered such that

$$v|_{x=l} = f(t) \quad (10)$$

Following Timoshenko[18], the dynamic displacement is composed of two parts:

$$v = v_I + v_{II} \quad (11)$$

where

$$v_I = \left[\frac{3m^2}{4} \left(\frac{x}{l} \right)^2 - \frac{m^2}{4} \left(\frac{x}{l} \right)^3 \right] f(t) \quad (12)$$

The term in the bracket represents the static mode function and satisfies the end conditions:

$$v_I|_{x=0} = 0, \quad v_I|_{x=l} = 0, \quad \frac{dv_I}{dx}|_{x=0} = 0, \quad \frac{d^2 v_I}{dx^2}|_{x=l} = 0 \quad (13)$$

but not the dynamic equation of motion:

$$EI \frac{d^4 v}{dx^4} + \rho A \frac{d^2 v}{dt^2} = 0 \quad (14)$$

Where EI and ρ are the flexural rigidity and density of the beam respectively,

The displacement v_I produces the dynamic loads as given by

$$-A \rho \left[\frac{3m^2}{4} \left(\frac{x}{l} \right)^2 - \frac{m^2}{4} \left(\frac{x}{l} \right)^3 \right] \ddot{f}(t) \quad (15)$$

Where A is the cross-sectional area of the beam

Moreover, the displacement (v_{II}) representing vibrations produced by the force function (15) is expressed as

$$v_{II} = \sum_i \phi_i(t) X_i(x) \quad (16)$$

where $X_i(x)$ and $\phi_i(t)$ are the modal and time-dependent functions, respectively.

v_{II} must satisfy the end conditions:

$$v_{II}|_{x=0} = 0, \quad v_{II}|_{x=l} = 0, \quad \frac{dv_{II}}{dx}|_{x=0} = 0, \quad \frac{d^2 v_{II}}{dx^2}|_{x=l} = 0 \quad (17)$$

$X_i(x)$ are the solutions of the expression (14) and satisfies the end condition as given in (17). Thus we get:

$$X_i = \sinh k_i l \operatorname{sink}_i(1-x) - \operatorname{sink}_i l \sinh k_i(1-x) \quad (18)$$

Where k_i are the roots of the following expression:

$$\tanh k_i l = \tan k_i l \quad (19)$$

The total displacement is then given by

$$V = \left[\frac{3m^2}{4} \left(\frac{x}{l} \right)^2 - \frac{m^2}{4} \left(\frac{x}{l} \right)^3 \right] f(t) + \sum_i \phi_i(t) X_i(x) \quad (20)$$

By applying the principle of virtual work, Timoshenko [18] has shown that the time-dependent functions must satisfy the differential equation given by

$$\frac{d^2 \phi_i}{dt^2} + \frac{E I k_i^4}{\rho A} \phi_i = b_i \frac{d^2 f(t)}{dt^2} \quad (21)$$

The coefficients b_i are obtained by expanding the force function (15) in a series of the normal functions, X_i . Thus,

$$-A \rho \frac{d^2 f(t)}{dt^2} \left[\frac{3m^2}{4} \left(\frac{x}{l} \right)^2 - \frac{m^2}{4} \left(\frac{x}{l} \right)^3 \right] = -A \rho \frac{d^2 f(t)}{dt^2} \sum_i b_i X_i \quad (22)$$

The coefficients b_i are obtained from the following expression:

$$b_i = \frac{\int_0^l \{x_i\} \left[\frac{3m^2}{4} \left(\frac{x}{l} \right)^2 - \frac{m^2}{4} \left(\frac{x}{l} \right)^3 \right] dx}{\int_0^l x_i^2 dx} \quad (23)$$

Integrating the expression (23) b_i is finally found to be:

$$b_i = \frac{m^2}{k_i l (\sinh k_i l - \sin k_i l)} \quad (24)$$

The general solution of expression (21) is given by

$$\varphi_i(t) = A_i \cos p_i t + B_i \sin p_i t - \frac{b_i}{p_i} \int_0^t \dot{f}(t) \sin p_i(t - \tau) d\tau \quad (25)$$

Where

$$p_i = \left(\frac{EI}{A\rho}\right)^{1/2} k_i^2$$

Constants A_i and B_i are evaluated from the initial conditions

$$v(0) = U(x, 0) \quad (26a)$$

$$\frac{dv(0)}{dx} = V(x, 0) \quad (26b)$$

Putting expression (20) in (26), U and V are evaluated as

$$U = \left[\frac{3m^2}{4} \left(\frac{x}{l}\right)^2 - \frac{m^2}{4} \left(\frac{x}{l}\right)^3 \right] f(0) + \sum_i A_i X_i \quad (27a)$$

$$V = \left[\frac{3m^2}{4} \left(\frac{x}{l}\right)^2 - \frac{m^2}{4} \left(\frac{x}{l}\right)^3 \right] \dot{f}(0) + \sum_i X_i \{B_i P_i\} \quad (27b)$$

Moreover, from the expression we get:

$$\left[\frac{3m^2}{4} \left(\frac{x}{l}\right)^2 - \frac{m^2}{4} \left(\frac{x}{l}\right)^3 \right] = \sum_i b_i X_i \quad (28)$$

Putting expression (28) in (27) and simplifying we get:

$$U(x, 0) = \sum_i X_i \{A_i + b_i f(0)\} \quad (29a)$$

$$V(x, 0) = \sum_i X_i \{B_i P_i + b_i \dot{f}(0)\} \quad (29b)$$

Putting the initial conditions $U = V = 0$, the constants A_i and B_i are found as :

$$A_i = -b_i f(0) \quad (30a)$$

$$B_i = -\frac{b_i}{p_i} \dot{f}(0) \quad (30b)$$

Substitution of expressions (25) and (26) in (20) yields:

$$V(x,t) = \left[\frac{3m^2}{4} \left(\frac{x}{l}\right)^2 - \frac{m^2}{4} \left(\frac{x}{l}\right)^3 \right] f(t) - f(0) \sum_i b_i X_i \cos p_i t - \dot{f}(0) \sum_i \frac{b_i}{p_i} X_i \sin p_i t - \sum_i \frac{b_i}{p_i} X_i \int_0^t \dot{f}(t) \sin p_i(t-\tau) d\tau \quad (31)$$

Integrating and simplifying the expression (31), the transverse deflection is finally found to be:

$$V(x,t) = \left[\frac{3m^2}{4} \left(\frac{x}{l}\right)^2 - \frac{m^2}{4} \left(\frac{x}{l}\right)^3 \right] f(t) - \sum_i b_i X_i f(t) + \sum_i b_i X_i P_i \int_0^t f(\tau) \sin p_i(t-\tau) d\tau \quad (32)$$

2) Evaluation of Relative Dynamic Slip

The relative displacement for even and odd numbers of laminates, at any axial position “ x ” has been evaluated considering the in plane bending stresses and the curvature of the bent cantilever beam.

The relative slip for the even number of laminates is given by :

$$\Delta U = \frac{1}{E} \int_0^l 2(m-1) \sigma_x dx + 2(m-1) \frac{h}{m} \frac{dv}{dx} \quad (33)$$

Where σ_x is the in-plane bending stress.

From the force equilibrium, the in-plane bending stresses in the respective laminates are computed as follows:

$$\sigma_x = \frac{m\mu p(l-x)}{2h} \quad (34)$$

where p is the interface pressure evaluated using the expression (1).

Combining expressions (32), (33) and (34) and simplifying, the relative slip displacement at the interfaces for even number of laminates is given by

$$\Delta U_x = \frac{mh}{2Rl} [3(m-1)f(t) - (m-2)Q] \left[\frac{2x}{l} - \frac{x^2}{l^2} \right] + h \sum_i b_i k_i [\text{Sinh} k_i l \text{Cos} k_i(l-x) - \text{Sink}_i l \text{Cosh} k_i(l-x)] \times [f(t) - p_i \int_0^t f(\tau) \sin p_i(t-\tau) d\tau] \quad (35)$$

The relative slip for the odd number of laminates is given by

$$\Delta U = \frac{1}{E} \int_0^l 2(m-2) \sigma_x dx + 2(m-1) \frac{h}{m} \frac{dv}{dx} \quad (36)$$

Combining expressions (32), (33) and (34) and simplifying, the relative slip displacement at the interfaces for odd number of laminates is given by

$$\Delta U_x = \frac{mh}{2Rl} [-(m-2)Q + 3(m-1)f(t)] \left[\frac{2x}{l} - \frac{x^2}{l^2} \right] + h \sum_i b_i k_i [\text{Sinh} k_i l \text{Cos} k_i(l-x) - \text{Sink}_i l \text{Cosh} k_i(l-x)] \times [f(t) - p_i \int_0^t f(\tau) \sin p_i(t-\tau) d\tau] \quad (37)$$

3) Analysis of Energy Dissipation

The energy is dissipated due to friction and relative dynamic slip at the interfaces. For completely reversed loading, the product of the shear force, μp , and the relative displacement, Δu , is integrated over the length of the beam which is found to be equal to one-fourth of the energy dissipation in a complete cycle. Thus, energy dissipation per cycle as established by Goodman and Klumpp[6] is given by

$$E_{\text{loss}} = 4b \int_0^l \tau_{xy} \Delta u(x) dx = 4\mu p b \int_0^l \Delta u(x) dx \quad (38)$$

Substituting the expression (35) in (38) and integrating, the energy dissipation per cycle for even number of laminates is given by

$$E_{\text{loss}} = \frac{8(m-1)Q}{m} \left[f(t) - \frac{m^2 Q}{6R} \right] \quad (39a)$$

$$E_{\text{loss}} = \frac{8(m-1)Q}{m} [f(t) - V_{ce}] \quad (39b)$$

Where $V_{ce} = \frac{m^2 Q}{6R} = \frac{m^2(\mu p b h)}{6R}$ is the critical amplitude of excitation in even number of bolted beams;

$$E_{\text{loss}} = \frac{8(m-1)Q}{mR} \left[Rf(t) - \frac{m^2 Q}{6} \right] \quad (39c)$$

$$E_{\text{loss}} = \frac{8(m-1)Q}{mR} [Rf(t) - P_{ce}] \quad (39d)$$

Where $P_{ce} = \frac{m^2 Q}{6} = \frac{m^2(\mu p b h)}{6}$ the critical load in even number of bolted beams.

Substituting the expression (37) in (38) and integrating, the energy dissipation per cycle for odd number of laminates is given by

$$E_{\text{loss}} = \frac{8(m-1)Q}{m} \left[f(t) - \frac{m^2(m-2)Q}{6(m-1)R} \right] \quad (40a)$$

$$E_{\text{loss}} = \frac{8(m-1)Q}{m} [f(t) - V_{co}] \quad (40b)$$

Where $V_{co} = \frac{m^2(m-2)Q}{6(m-1)R} = \frac{m^2(m-2)\mu p b h}{6(m-1)R}$ is the critical amplitude of excitation in odd number of bolted beams;

$$E_{\text{loss}} = \frac{8(m-1)Q}{mR} \left[Rf(t) - \frac{m^2(m-2)Q}{6(m-1)} \right] \quad (40c)$$

$$E_{\text{loss}} = \frac{8(m-1)Q}{mR} [Rf(t) - P_{co}] \quad (40d)$$

Where $P_{co} = \frac{m^2(m-2)Q}{6(m-1)} = \frac{m^2(m-2)\mu p b h}{6(m-1)}$ is the critical load in even number of bolted beams.

Critical load is the minimum initial load applied to result in the energy loss due to friction at the interfaces. In other words, critical load is the minimum initial load needed to initiate the relative dynamic slip at the interfaces that will result in the energy dissipation due to dynamic slip and interface friction. From the expression for critical load it is quite obvious that it is dependent on the number of layers and interface pressure. With the increase in number of layers, the critical load is raised therefore greater load is needed to initiate the relative dynamic slip at the interface as compared to the two layered and welded beams. Also, with the increase in interface pressure critical load is raised along

with the friction force thereby reducing the relative slip at the interfaces and thus lowering the energy dissipation at the interfaces as evident from the expressions (39) and (40). Moreover, at high interface pressure there is a chance that the transition from the slip to stick phenomenon thereby resulting in sticking at the interfaces and resulting in no energy dissipation due to friction at the interfaces. It is very difficult to ascertain this transition limit or zone theoretically. However, this limit can be ascertained with rigorous experimental procedure which is not in the scope of the present work as the present analysis of the beam specimens is welded and the interface pressure developed due to assembling and welding is constant and cannot be varied as in the case of bolted beams where the pressure can be varied by tightening of the bolts.

Critical amplitude is the minimum initial amplitude of excitation required to result in the energy loss due to friction at the interfaces. In other words, critical amplitude can be defined as the minimum initial excitation needed to initiate the relative dynamic slip at the interfaces which will result in the energy dissipation due to dynamic slip and interface friction.

4) Evaluation of loss factor

In vibration problems, it is most convenient to express the dissipative properties of the system in terms of non-dimensional quantities such as the loss factor “ η_s ”, defined by:

$$\eta_s = \frac{E_{loss}}{2\pi E_{ne}} \quad (41)$$

Where, E_{ne} is the maximum strain energy stored in the system. The maximum strain energy stored in the system in terms of dynamic deflection at the tip of the beam is given by

$$E_{ne} = \frac{1}{4R} \left(\frac{Rf(t)}{2} + Q \right)^2 \quad (42)$$

Putting expressions (39) and (42) in expression (41) and simplifying, the loss factor in terms of dynamic tip displacement for even number of laminates is given by

$$\eta_s = \frac{64(m-1) \left[\frac{Rf(t)}{Q} - \frac{m^2}{6} \right]}{m\pi \left(\frac{Rf(t)}{Q} + 2 \right)^2} \quad (43)$$

Putting expressions (40) and (42) in expression (41) and simplifying, the loss factor in terms of dynamic tip displacement for odd number of laminates is given by

$$\eta_s = \frac{64(m-1) \left[\frac{Rf(t)}{Q} - \frac{m^2(m-2)}{6(m-1)} \right]}{m\pi \left(\frac{Rf(t)}{Q} + 2 \right)^2} \quad (44)$$

III. EXPERIMENTAL SETUP

A. Preparation of Specimen

The test specimens of different sizes are prepared from the same stock of commercial mild steel flats as presented in Tables. Equi-spaced bolts of diameter 12 mm are used to fabricate two and multi layered specimens. The distance between the consecutive connecting bolts have been kept as 3.5 times their diameter depending on the diameter of the connecting bolts. The cantilever lengths of the specimens have been varied accordingly in order to accommodate the corresponding number of connecting bolts as presented in table.



(a)



(b)

Fig. 2: Figure of mild steel specimen (a). of length 378mm (b). of length 588mm.

Dimension of the specimen (thickness × width), (mm×mm)	Number of layers used	Number of bolts used	Cantilever length (mm)	Types of joints
3.00×40.00	2	9	378	Bolted
3.00×40.00	3	9	378	Bolted
3.00×40.00	4	9	378	Bolted
3.00×40.00	2	14	588	Bolted
3.00×40.00	3	14	588	Bolted
3.00×40.00	4	14	588	Bolted
6.00×40.00	2	9	378	Bolted
6.00×40.00	3	9	378	Bolted
6.00×40.00	4	9	378	Bolted
6.00×40.00	2	14	588	Bolted
6.00×40.00	3	14	588	Bolted
6.00×40.00	4	14	588	Bolted

Table 1: Details of mild steel specimens used for layered and bolted beams.

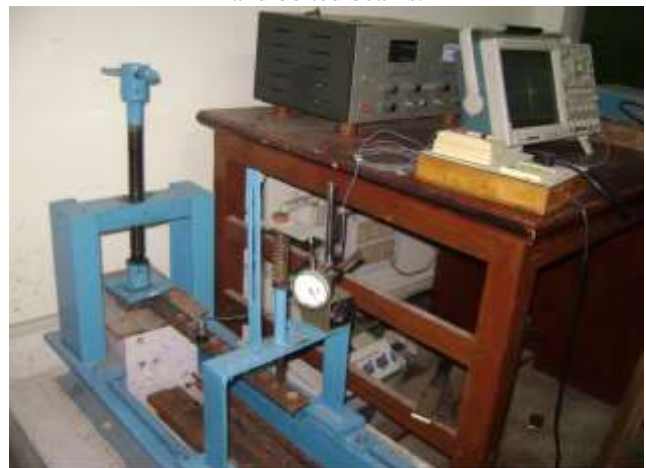


Fig. 3: Experimental setup.

B. Experimental Procedure

In order to validate the developed mathematical model for the loss factor of layered and tack welded mild steel beams experiments have been conducted. An experimental setup as shown in Fig.3 has been fabricated to conduct the experiments. Experiments have been conducted to evaluate experimental loss factor for welded beams of various configurations vibrating at dynamic conditions The

cantilever specimens are excited transversally at the amplitudes of 0.1, 0.2, 0.3, 0.4 and 0.5 mm at their free ends with the help of an exciter. The input excitation and output vibration are sensed with vibration pick-ups and the corresponding signal is fed to a digital storage oscilloscope. The test specimens are fixed at one end with the help of mechanical vice as shown in Fig.3. Proper care has been taken to ensure perfect cantilever condition. The vibration generator is placed at the driving point just below the free end of the cantilever specimen.

C. Measurement of Young's Modulus of Elasticity (E)

As mentioned in the preceding paragraph, the Young's modulus of elasticity (E) of the specimen material is found out by conducting static deflection tests. For this purpose specimens are mounted on the same experimental set-up rigidly so as to ensure perfect fixed boundary conditions as mentioned earlier. Static loads (W) are applied at the free end and the corresponding deflections (Δ) are recorded. The Young's modulus for the specimen material is determined using the expression $E = \frac{Wl^3}{I\Delta}$, where l and I are the free length and moment of inertia of the cantilever specimen. The average of five readings is recorded from the tests from which the average value of Young's modulus for different material is found to be 196.0 (GPa).

D. Measurement of Static Bending Stiffness (k)

It is a well known fact that the stiffness of a jointed beam is always less compared to an equivalent solid one. It means that the incorporation of joints to assemble layers of beams is accompanied by a decrease in the stiffness. The amount of reduction in the stiffness is quantified by a factor called stiffness ratio which is defined as the ratio of the stiffness of a jointed beam (k) to that of an identical solid one (k'). The same static deflection tests as used in case of Young's modulus are performed to measure the actual stiffness (k) of a jointed specimen using the relation $k = W/\Delta$.

E. Measurement of Damping (δ)

After finding out the Young's modulus and static bending stiffness of the specimen materials, the tests are further conducted on the same set of specimens for evaluating the logarithmic decrement. The test specimens are first rigidly mounted on the set-up one after another. The test procedure is essentially the same for all the cases. The excitation is imparted for a range of beam-tip amplitudes varying from 0.1 to 0.5 mm in steps of 0.1 mm. The decaying signal is recorded on the screen of the storage oscilloscope indicating that the energy dissipation is taking place. The cause of energy dissipation may be due to different effects such as material, joint friction and support damping. However, it is assumed that all the energy dissipation is due to the joint friction only. The value of logarithmic decrement can be calculated by using relation:

$$\delta = \frac{1}{n} \ln \left(\frac{a_1}{a_{n+1}} \right)$$

Where

a_1 = amplitude of first cycle

a_{n+1} = amplitude of last cycle and

n = no. of cycles.

IV. RESULT AND DISCUSSION

The variation of dynamic response of the cantilever specimen at various distances from the fixed end ($x = 0$ to l) has been plotted in Fig.4. From the figure it is inferred that the dynamic response increases with the distance from the fixed end and is maximum at the unsupported end.

The variation of relative slip with axial distance from the fixed end has been plotted in Fig.5. From the figure it is quite evident that the relative slip increases with the distance from the fixed end and is maximum at the free end also the small increase is obtained with number of layers.

From Figs 6 and 7 it is evident that the loss factor decreases with increase in initial amplitude excitation at the free end of the beam model and thickness of laminates .

From Fig.8 it is concluded that the logarithmic decrement increases with increase in the number of laminates and also increases with overall length of the beam.

The variation of energy dissipation with the initial amplitude of excitation for the layered and jointed beams for Heaviside and harmonic loadings has been plotted in Fig.9. From the figure it is apparent that the energy dissipation increases with the increase in initial amplitude of excitation.

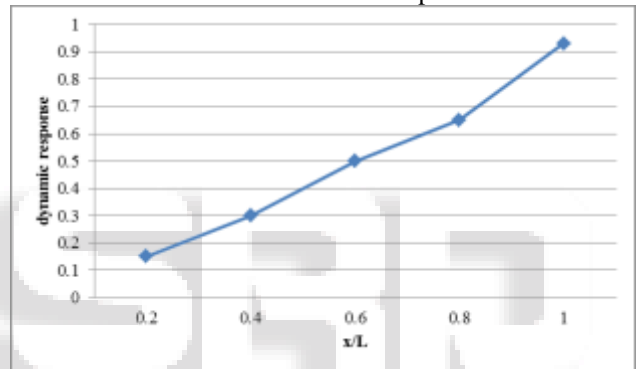


Fig. 4: variation of dynamic response with axial distance from fixed end

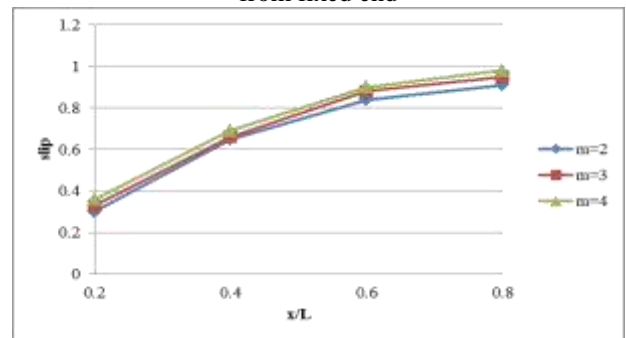


Fig. 5: Variation of relative slip with axial distance from free end for specimen of different number of layers.

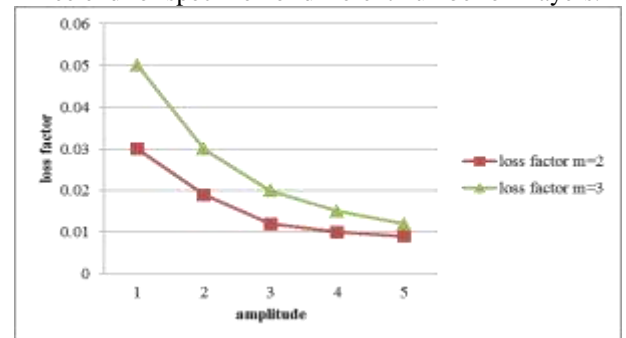


Fig. 6: variation of loss factor with respect to amplitude for m=2 and m=3.

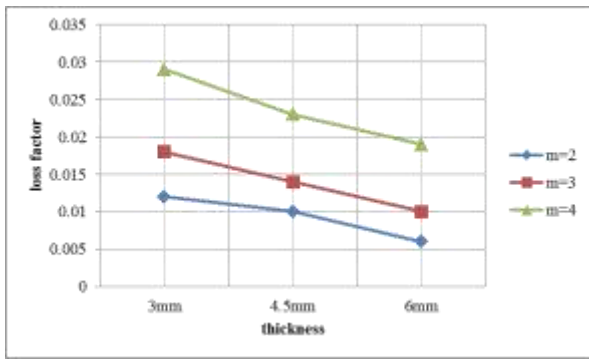


Fig. 7: variation of loss factor with respect to thickness of laminates for different number of laminates for $m=2$ and $m=3$.

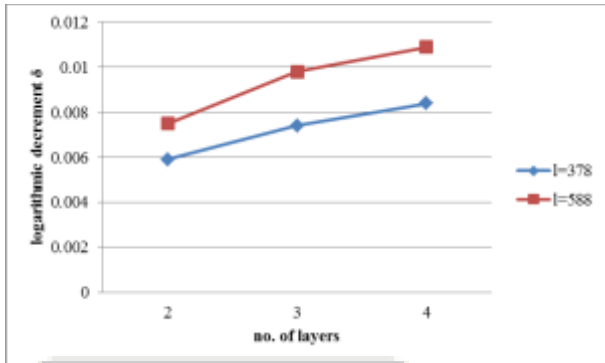


Fig. 8: variation of logarithmic decrement with respect to number of laminates for beams of different lengths.

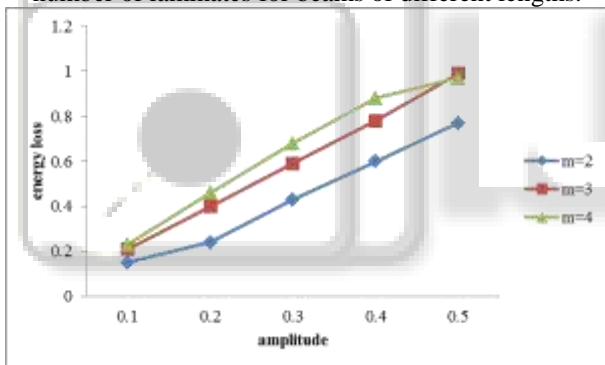


Fig. 9: Variation of energy loss with amplitude

V. CONCLUSION

In the present work, a mathematical analysis has been carried out to investigate the mechanism of slip damping with multiple interfaces. Experiments are conducted to validate the theory developed. From the results plotted, it is inferred that damping capacity of layered and welded structures can be substantially enhanced by fabricating the structures with multiple interfaces. Further, it is also deduced that the relative slip, length, thickness, and initial amplitude of excitation are the vital parameters influencing the damping capacity of fabricated structures.

REFERENCES

[1] Bhagat Singh, Bijoy Kumar Nanda, Dynamic analysis of damping mechanism in welded multilayered mild steel beams, *Aerospace science and technology* 29 (2013) 58-73.
[2] L. Heller, E.Foltete, J.Piranda, Experimental identification of nonlinear dynamic properties of built-

up structures, *Journal of Sound and Vibration* 327 (2009) 183–196.
[3] W. Chen, X. Deng, Structural damping caused by micro-slip along frictional interfaces, *International Journal of Mechanical Sciences* 47 (2005) 1191–1211.
[4] T.H.H. Pian, F.C. Hallowell, Investigation of structural damping in simple builtup beams, Technical Report, Contract N5ori-07833 to ONR, Aeroelastic and Structures Laboratory, Massachusetts Institute of Technology, Cambridge, Mass., 1950.
[5] B.K. Nanda, Study of the effect of bolt diameter and washer on damping in layered and jointed structures, *Journal of Sound and Vibration* 290 (2006) 1290–1314.
[6] L.E. Goodman, J.H. Klumpp, Analysis of slip damping with reference to turbine blade vibration, *Journal of Applied Mechanics* 23 (1956) 421.
[7] D.P. Hess, et al., Normal vibrations and friction at a Hertzian contact under random excitation: theory and experiment, *Journal of Sound and Vibration* 153 (3) (1992) 491–508.
[8] C. Cockerham, G.R. Symmons, Stability criterion for stick-slip motion using a discontinuous dynamic friction model, *Wear* 40 (1976) 113–120.
[9] A. Guyan, et al., Dynamics with Friction: Modeling, Analysis and Experiment, Series on Stability, Vibration and Control of Systems, World Scientific, Singapore, 1996.
[10] D.M. Barnett, et al., Slip wave along the interface between two anisotropic elastic half-spaces in sliding contact, *Proceedings of the Royal Society of London, Series A* 415 (1988) 389–419.
[11] G.A. Maugin, et al., Interfacial waves in the presence of areas of slip, *Geophysical Journal International* 118 (1994) 305–316.
[12] S.W. Hansen, R. Spies, Structural damping in laminated beams due to interfacial slip, *Journal of Sound and Vibration* 204 (2) (1997) 183–202.
[13] O. Damisa, V.O.S. Olunloyo, C.A. Osheku, A.A. Oyediran, Static analysis of slip damping with clamped laminated beams, *European Journal of Scientific Research* 17 (4) (2007) 455–476.
[14] O. Damisa, V.O.S. Olunloyo, V. Osheku, A.A. Oyediran, Dynamic analysis of slip damping in clamped layered beams with non-uniform pressure distribution at the interface, *Journal of Sound and Vibration* 309 (2008) 349–374.
[15] K.L. Johnson, *Contact Mechanics*, Cambridge University Press, New York, 1985.
[16] A.E. Giannakopoulos, T.C. Lindley, S. Suresh, C. Chenu, Similarities of stress concentrations in contact at round punches and fatigue at notches: Implications to fretting fatigue crack initiation, *Fatigue and Fracture of Engineering Material and Structures* 23 (7) (2000) 561–571.
[17] G.B. Warburton, *The Dynamical Behaviour of Structures*, 2nd ed., Pergamon Press Ltd., Oxford, England, 1976, pp. 204–205, 230–231.
[18] S. Timoshenko, *Vibration Problems in Engineering*, 3rd ed., Van Norstrand Co., Inc., 1955, p. 371.